Ahn et al. *NPG Asia Materials* (2022) 14:46
https://doi.org/10.1038/s41427-022-00387-3

NPG Asia Materials

ARTICLE Open Access

Combinatorial physicochemical stimuli in the three-dimensional environment of a hyaluronic acid hydrogel amplify chondrogenesis by stimulating phosphorylation of the Smad and MAPK signaling pathways

Jinsung Ahn[1], Yoshie Arai[1], Byoung Ju Kim[1], Young-Kwon Seo[1], James J. Moon[2], Dong Ah Shin[3], Bogyu Choi[4] and Soo-Hong Lee[1]

Abstract

The chondrogenesis of stem cells and cartilage tissue regeneration are more efficient in a three-dimensional (3D) environment than in a two-dimensional (2D) environment. Although extensive studies have examined the effects of biochemical or physical cues alone, it is not fully understood how these biochemical and biophysical cues in the 3D environment are intertwined and orchestrated with chondrogenesis for cartilage tissue regeneration. In this study, we used photocrosslinked hyaluronic acid (HA), the extracellular matrix of cartilage, as a general 3D microenvironment to characterize the effects of dimensionality, localization of biochemical cues, regulation of biophysical cues, and external stimulation on chondrogenic signaling pathways in adipose-derived stem cells (hASCs). TGF-β3 was immobilized in HA hydrogels by ionic or covalent conjugation. The stiffness of the hydrogels was tuned by varying the crosslinking density, and an external stimulus for chondrogenesis was provided by ultrasound. The results revealed that the levels of chondrogenic signals in hASCs cultured in the 3D HA hydrogel depended on the presence of TGF-β3, and a reduction in the stiffness of the TGF-β3 covalent conjugated hydrogel increased the chance of interaction with encapsulated hASCs, leading to an increase in chondrogenic signals. External stimulation with ultrasound increased the interaction of hASCs with HA via CD44, thereby increasing chondrogenesis. Our results present a new understanding of the intertwined mechanisms of chondrogenesis in 3D hydrogels connecting TGF-β3 sequestration, mechanical properties, and ultrasound-based external stimulation. Overall, our results suggest that when designing novel biomaterials for tissue engineering, it is necessary to consider the combinatorial mechanism of action in 3D microenvironments.

Introduction

The extracellular matrix (ECM) is a dynamic and complex three-dimensional (3D) microenvironment that continuously delivers biochemical and physical signals to cells within it[1,2]. To identify a novel stem cell niche for chondrogenic tissue engineering, many researchers have sought to understand the role of biochemical and biophysical factors in determining cellular behaviors,

Correspondence: Dong Ah Shin (shindongah@me.com) or Bogyu Choi (bgchoi725@gmail.com) or Soo-Hong Lee (soohong@dongguk.edu)
[1]Department of Medical Biotechnology, Dongguk University, 32 Dongguk-ro, Ilsandong-gu, Goyang, Gyeonggi 10326, Republic of Korea
[2]Department of Pharmaceutical Sciences, Department of Biomedical Engineering & Biointerfaces Institute, University of Michigan, Ann Arbor, MI 48109, USA
Full list of author information is available at the end of the article
These authors contributed equally: Dong Ah Shin, Bogyu Choi, Soo-Hong Lee.

especially stem cell differentiation. Through regulation of mechanical cues, it is possible to control the self-renewal and differentiation of stem cells[3–6]. In addition, the microenvironment can serve as a tool for biochemical, biophysical, and structural stimuli and their effects on stem cells[7,8]. Although 2D environment studies are useful for exploring the general principles underlying the regulation of cellular signaling pathways by biochemical and physical stimuli, it is critical to understand and recapitulate the complexity of 3D microenvironments[9]. To overcome this limitation, researchers have developed hydrogel systems as a model 3D microenvironment. Hydrogels composed of various materials are used to study the differentiation of adipose-derived stem cells and the regulation of stem cell fate[10,11]. Because these efforts have focused on individual stimuli, however, they have largely been limited to finding better 3D hydrogel systems or identifying physical cues suitable for specific types of differentiation[12–14]. Therefore, it remains unclear whether the mechanisms of chondrogenic differentiation in 3D environments, especially those that provide multiple combinatorial stimuli, are similar to those in 2D environments.

Growth factors are often introduced as critical factors in culture media during in vitro experiments; however, in vivo conditions are unique in that growth factors are sequestered in the ECM, enabling local presentation to cells[15]. Accordingly, ongoing research has focused on how to develop biomimetic 3D microenvironments by sequestering and presenting biochemical factors, such as cytokines and growth factors, to cells encapsulated in 3D matrices for purposes related to stem cell culture, differentiation, and regenerative medicine[16,17]. Recently, a number of growth factors[18], such as vascular endothelial growth factor (VEGF)[19,20], platelet-derived growth factor (PDGF)[21,22], and transforming growth factor-beta (TGF-β)[23,24], have been immobilized in various scaffolds, including hydrogels, without negatively affecting their bioactivity. Among them, TGF-β plays a critical role in chondrogenic differentiation[25–27]. However, it remains unclear how the mechanism of action differs between soluble TGF-β3 and insoluble TGF-β3 immobilized onto ECM. In this study, by using photocrosslinkable hyaluronic acid (HA) hydrogels, we uncovered similarities and differences in TGF-β3/Smad[28] and MAPK signaling[29] during chondrogenic differentiation of human adipose-derived stem cells (hASCs) between 2D and 3D microenvironments[30,31]. Then, we evaluated the regulatory effects of 3D mechanical properties and external stimulation on these signaling pathways in hASCs encapsulated in 3D microenvironments. Although previous studies have examined the impact of stiffness on chondrogenic differentiation in 2D environments[32,33], it remains unclear how the mechanical stiffness of hydrogels influences chondrogenic differentiation in 3D culture. Using the HA-based hydrogel system, we found that mechanical stiffness indeed affects 3D hydrogels. Previous studies reported that HA hydrogel stiffness associated with CD44-mediated mechanosensitive signaling regulates cell adhesion, migration, and the multipotency of MSCs[34–36]. In addition, various types of external stimuli, such as near-infrared radiation, dynamic compression, and hydrostatic pressure, have been used in chondrogenic differentiation[37–41]. For the experimental paradigm in this study, we chose ultrasound (US) stimulation, which has been widely used for human clinical trials[42,43]. US increases the level of ECM cartilage components and expression of cartilage-related genes[44,45]. US stimulation-induced proteoglycan expression and chondrocyte migration and proliferation. Furthermore, ultrasound increased chondrogenic differentiation markers. Overall, these findings provide a new framework for understanding how biochemical and biophysical cues, coupled with external stimulation, impact chondrogenic differentiation of hASCs within 3D hydrogels.

Results and discussion

The 2-dimensional vs. 3-dimensional environment of chondrogenic differentiation

Initially, to investigate the effect of microenvironmental dimensionality on the integrated mechanism of chondrogenesis, we used HA to provide a chondrogenic microenvironment for the cells[46]. For these experiments, HA was modified with methacrylic anhydride to yield photocrosslinkable methacrylated HA, which enabled the formation of a crosslinked hydrogel network following irradiation with UV (365 nm) in the presence of a photoinitiator, Irgacure 2959 (Fig. 1a)[47]. First, we induced chondrogenesis of hASCs in 3D HA hydrogels and compared the expression of chondrogenic markers and signaling pathway proteins with those in the hASCs cultured on 2D TC plates (Fig. 1b). For the 3D hydrogel, methacrylated hyaluronic acid (MAHA) with a degree of substitution (DS) of 50 was used. The addition of TGF-β3 to the chondrogenic media for 2 weeks during 2D and 3D culture of hASCs (2D + T and 3D + T groups) led to upregulation of chondrogenic gene expression (Fig. 1c). In particular, the mRNA levels of *SOX9* and *ACAN* in the 3D + T group were 1.3-fold and 1.6-fold higher, respectively, than those in the 2D + T group. Continuous addition of TGF-β3 in chondrogenic media significantly increased the gene expression levels of *COL10*, a hypertrophic marker, and *COL1A1*, a fibroblastic and osteogenic marker, in both the 2D and 3D systems. However, the mRNA levels of *COL10* and *COL1A1* in the 3D + T group were significantly lower than those in the 2D + T group (6.6-fold and 1.3-fold, respectively), indicating that hASCs cultured in hydrogels in the presence of TGF-β3

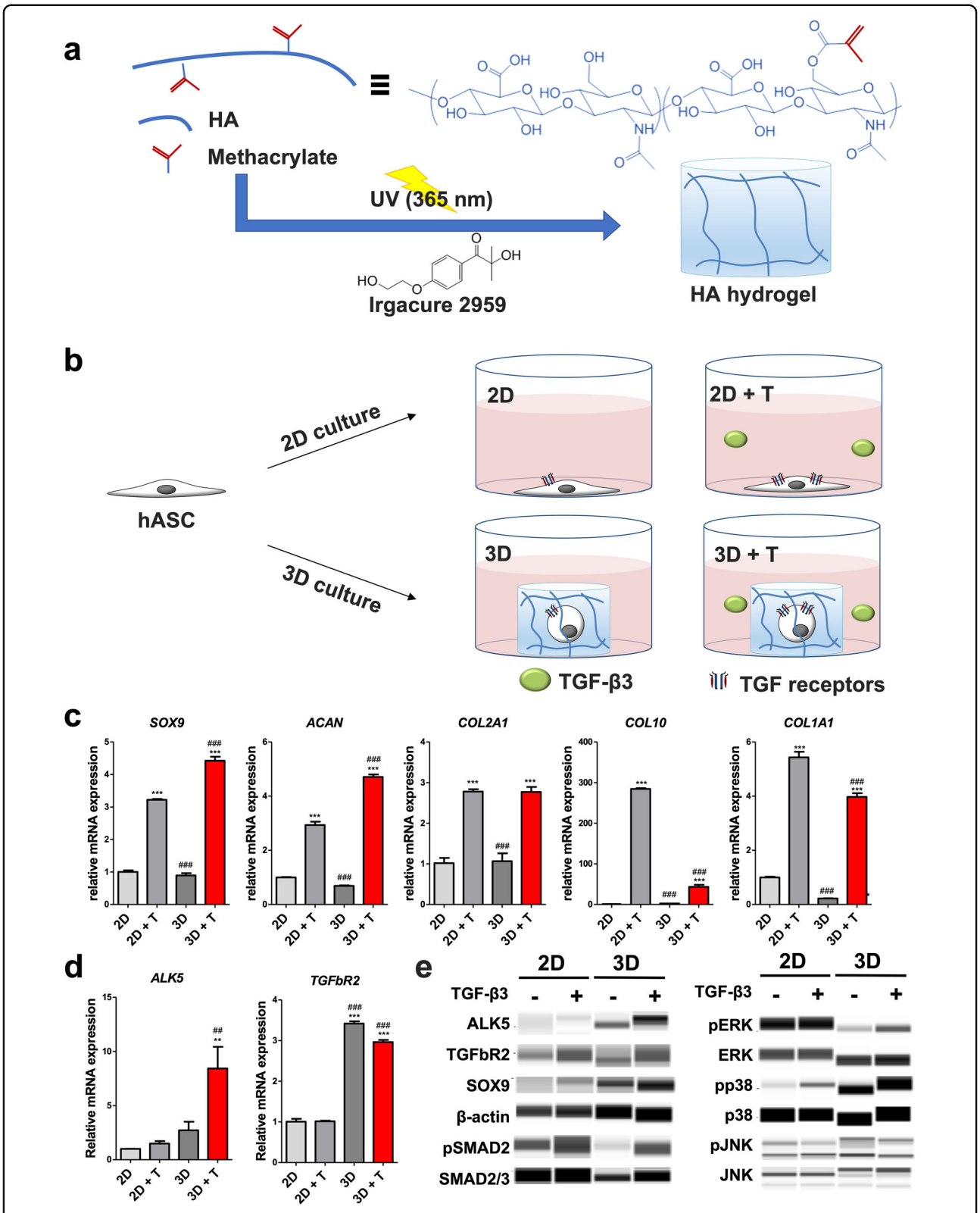

Fig. 1 Effect of microenvironment dimensionality on chondrogenesis by human adipose-derived stem cells (hASCs). a Schematic diagram of HA hydrogel. **b** Schematic representation of chondrogenesis by hASCs in 2D and 3D culture. DS50 of MAHA was used as a 3D hydrogel. **c** Chondrogenic gene expression, **d** TGF-β ligand gene expression, and **e** protein expression in hASCs undergoing chondrogenesis in 2D and 3D environments. ($n = 5$; $^{*}P < 0.05$, $^{**}P < 0.01$, $^{***}P < 0.001$ vs. 2D; $^{\#}P < 0.05$, $^{\#\#}P < 0.01$, $^{\#\#\#}P < 0.001$ vs 2D + TGF-β3).

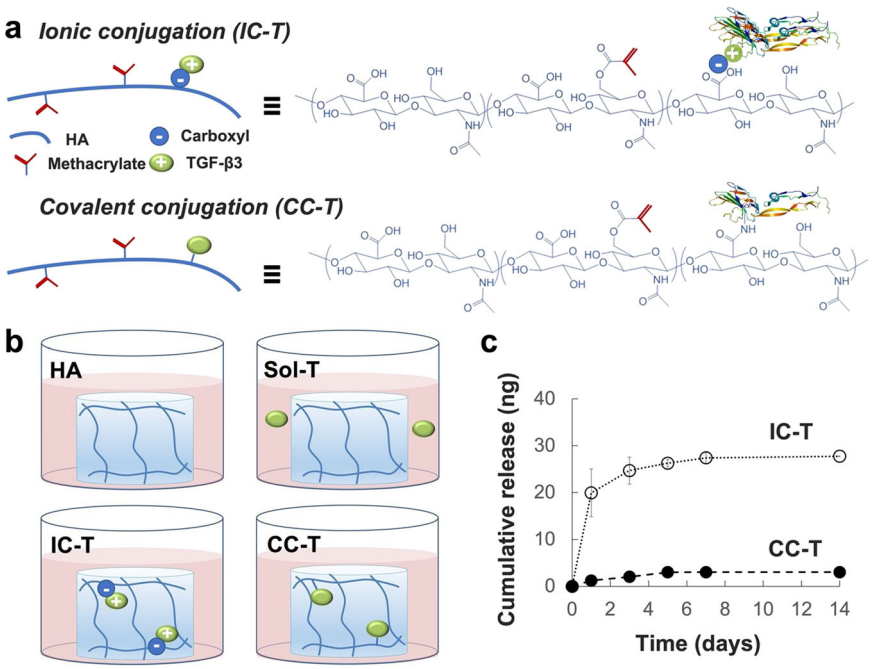

Fig. 2 Preparation of bioinspired 3D microenvironments for cartilage tissue engineering by sequestration of TGF-β3. a Ionic and covalent conjugation scheme for sequestration of TGF in the HA hydrogel. **b** Schematic illustration of 3D culture. **c** TGF-β3 release profile over 14 days, as determined by ELISAs ($n = 4$).

can effectively inhibit the expression of hypertrophic and osteogenic markers. Encapsulating cells in hydrogels can suppress the expression of hypertrophic, fibroblastic and osteogenic markers. Therefore, it is more suitable to use a 3D system that lowers the expression of *COL1A1* and *COL10* to induce hyaline cartilage[48]. In most cells, TGF-β ligands bind to the TGF-β type II receptor (TGFbR2), which then recruits the type I receptor, activin-like kinase 5 (ALK5), to activate the SMAD signaling pathway[49,50]. We found that *TGFBR2* expression in hASCs was much higher in 3D than in 2D culture, but the addition of TGF-β3 to the culture medium did not cause a significant difference in either system (Fig. 1d). Interestingly, we observed a significant increase in *ALK5* expression only in the 3D + T group.

Next, we examined the phosphorylation of Smad and MAPK proteins, which are components of signaling pathways involved in chondrogenesis. The protein levels of ALK5, SOX9, phospho-SMAD2 (pSMAD2), and phospho-p38 (pp38) were upregulated by the addition of TGF-β3 to the culture medium in both the 2D and 3D systems (Fig. 1e). The phosphorylation of ERK increased in the presence of TGF-β3 only in the 3D system and was high regardless of TGF-β3 in the 2D system. The levels of pp38 were significantly higher in the 3D system than in the 2D system. Previous works have shown that a 3D environment improves chondrogenic differentiation efficiency[51,52]. Our findings demonstrated that the 3D HA hydrogel increases chondrogenic differentiation efficiency by amplifying the p38 pathway.

Biochemical effects of the HA hydrogel on chondrogenic differentiation in a 3D environment

To prepare bioinspired 3D microenvironments for cartilage tissue engineering, we introduced TGF-β3, a chondrogenic biochemical factor, into HA hydrogels through ionic or covalent conjugation. The protonated amino groups of Arg and Lys in TGF-β3 at physiological pH can engage in ionic conjugation with deprotonated carboxyl groups in methacrylated HA (IC-T) (Fig. 2a). Several receptor-binding ligands (e.g., BMPs and TGFs) interact with cell-surface receptors in substrate-immobilized forms to trigger signal transduction and cellular responses[53,54]. To localize TGF-β3 near encapsulated hASCs, we covalently conjugated TGF-β3 to the backbone of methacrylated HA using EDC/NHS chemistry (CC-T). Specifically, the free amino groups in TGF-β3 could form amide bonds by reacting with the NHS-activated carboxyl group in methacrylate HA. The HA hydrogel lacking TGF-β3 was used as a negative control, and the HA hydrogel with unconjugated free TGF-β3 in chondrogenic media (Sol-T) was used as a positive control for the TGF-β3–conjugated groups (IC-T and CC-T) (Fig. 2b). Eighty nanograms of TGF-β3 were loaded, and the release amount was confirmed under DPBS conditions for 14 days. The release profile was measured on Days 1, 3, 5,

7, and 14, and DPBS was replaced according to the measured data. The release profile of sequestered TGF-β3 from hydrogels in DPBS conditions revealed that 25% of the initially loaded TGF-β3 in IC-T was released in 1 day, followed by a slower release, resulting in a cumulative release of 36% by Day 14. In contrast, only 3.7% of TGF-β3 was released from CC-T cells by Day 14 (Fig. 2c, Fig. S1, Supporting Information). This sustained release of TGF-β3 from IC-T may be due to the reversible affinity binding of positively charged amino acids in TGF-β3, such as Lys and Arg, to negatively charged carboxyl groups in HA. TGF-β3 in IC-T showed a release pattern from the hydrogel that was relatively higher than that in CC-T. A previous study showed that electrostatic binding of TGF-β1 to collagen II is unstable in the presence of serum proteins and cells in crosslinked hydrogels[53], suggesting that the CC-T system would be preferable to the IC-T system. Therefore, we believe that CC-T would improve chondrogenesis more than IC-T. The existence of TGF-β3 sequestered by covalent conjugation was confirmed by immunostaining of TGF-β3 after 14 days of incubation; the results confirmed that covalently conjugated TGF-β3 was still in the 3D hydrogel until the end of the incubation time (Fig. S2, Supporting Information). These experiments demonstrate the impact of various conjugation strategies and reveal that TGF-β3 immobilized in 3D hydrogels via covalent conjugation preserves its bioactivity while allowing sustained drug release. Overall, the covalent conjugation system more effectively retained TGF-β3 in the HA hydrogel.

Next, we sought to determine the effects of sequestering TGF-β3 on the chondrogenic differentiation of encapsulated hASCs and to characterize the underlying mechanism. To this end, we encapsulated hASCs in the TGF-β3-sequestered hydrogels (IC-T and CC-T groups) and compared them with the hASCs in HA with (Sol-T group) or without (HA group) TGF-β3 in the culture media. In the IC-T and CC-T groups, in which TGF-β3 was sequestered in a 3D microenvironment, the expression of hyaline cartilage-specific markers (chondroitin sulfate and type II collagen) was significantly higher than that in the HA group and as high as that in the Sol-T group (Fig. 3a). Next, we measured the expression of genes encoding chondrogenic markers. The mRNA levels of *SOX9*, *ACAN*, and *COL2A1* in CC-T cells were 10-, 3-, and 1.7-fold higher than those in HA cells but lower than those in Sol-T cells (Fig. 3b). In addition, the expression of the hypertrophic and osteogenic markers *COL10* and *COL1A1* with TGF-β3 in the chondrogenic medium was inhibited by the encapsulation of hASCs in 3D hydrogels. In this comparison, the expression of *COL10* and *COL1A1* was even lower than that in the hASCs encapsulated in the TGF-β3–sequestered hydrogel systems (IC-T and CC-T). The quantitative content of sulfated glycosaminoglycan (sGAG) and collagen in hydrogels was consistent with the immunostaining results (Fig. 3c), but only the CC-T group exhibited a significant increase in collagen content. As shown in Fig. 1e, in 3D microenvironments, the level of *TGFbR2* was not dependent on the presence of TGF-β3, whereas the level of *ALK5* was dependent on the presence of TGF-β3 (Fig. 3d). As expected, because the same concentration of HA was used for all hydrogels, the expression of *CD44*, a receptor for HA, did not differ among the groups (Fig. 3e). As shown in Fig. 1e, elevated expression of pSMAD2, pERK, ALK5, and SOX9 was observed in the presence of added or sequestered TGF-β3, whereas the pJNK level was not significantly altered (Fig. 3f). The expression of pERK, pp38, SOX9, and ALK5 was significantly upregulated in the TGF-β3 sequestration systems (IC-T and CC-T) compared with that of Sol-T. Remarkably, the expression of ALK5 and SOX9 was highest in the CC-T group. These data indicate that localizing TGF-β3 around encapsulated hASCs can easily trigger chondrogenesis via both the Smad and non-Smad pathways.

Biochemical effects on cartilage regeneration in the chondral defect model

Next, we investigated the feasibility of TGF-β3-sequestering hydrogels to support cartilage regeneration in a rat partial-thickness chondral defect model. Given the small size of the joints, the thinness of the articular cartilage, and high intrinsic healing potential in the rodent model[55–57], we created partial-thickness chondral defects that were not exposed to bone marrow-derived MSCs or bone marrow elements[53,58,59]. To investigate the cartilage regeneration effect in the chondral defect model, we performed in vivo studies with 10- to 12-week-old SD rats[60–62]. Although the rats are still growing, knee cartilage analysis has been carried out between 4 and 24 weeks after surgery[63,64]. In this study, we investigated the cartilage regeneration effect at the defect site 8 weeks after implantation (Fig. 4). This evaluation revealed that defects treated with hASCs encapsulated in TGF-β3-sequestered hydrogels (IC-T + hASCs and CC-T + hASCs) were covered with integration to the surrounding native cartilage without apparent inflammation, whereas defect sites that were untreated (defect) or treated with hASCs encapsulated in hydrogel without TGF-β3 (HA + hASCs) had rough surfaces that were morphologically distinct from the surrounding cartilage (Fig. 4a). To observe differences in the cellular structure and matrix composition between the different implantation groups, we performed histological analysis by staining with Safranin O for sGAG, Masson's trichrome for collagen, and immunohistochemistry (IHC) for type II collagen (Fig. 4b), followed by quantitative evaluation. The defect and HA + hASC groups exhibited incomplete defect

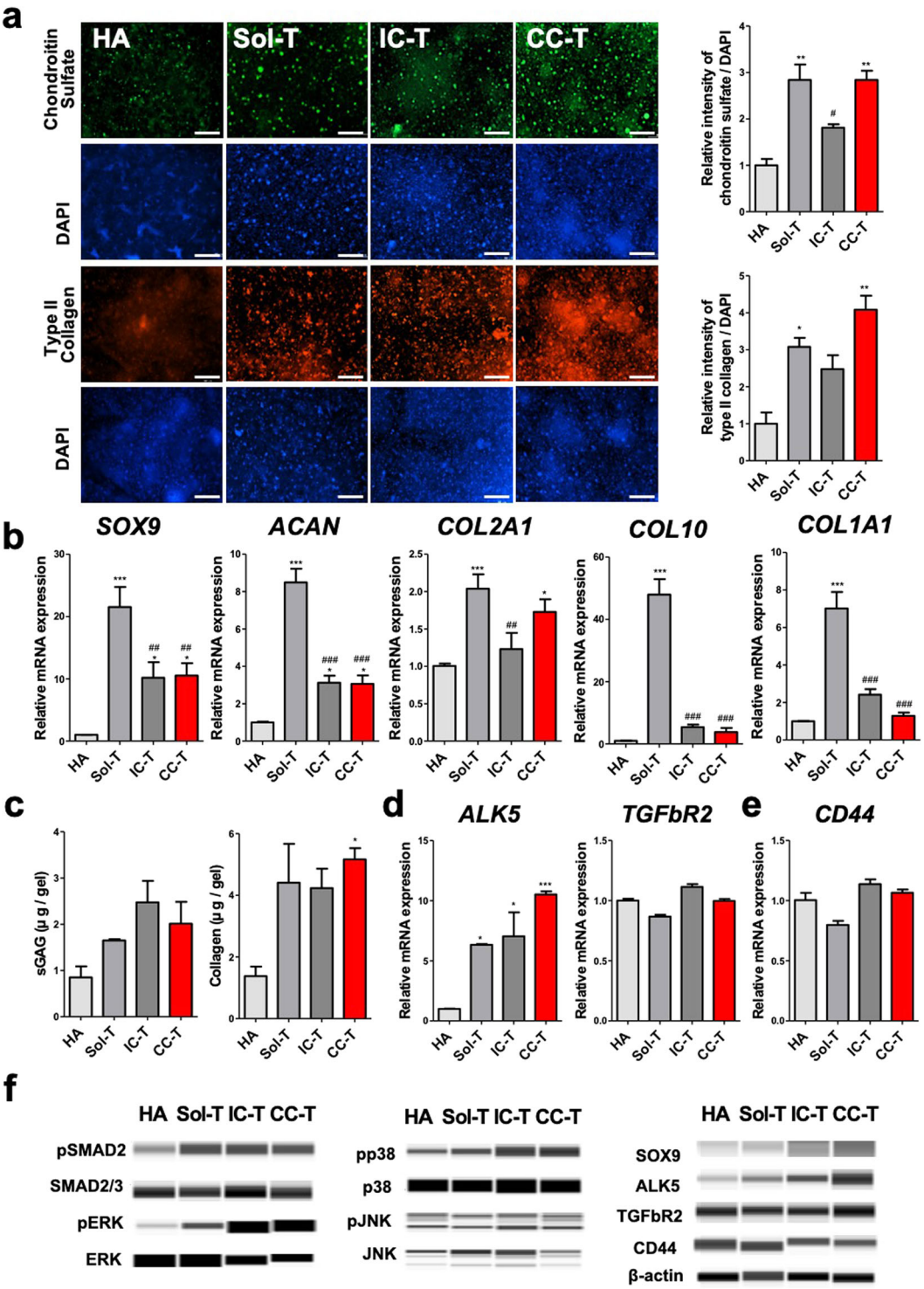

Fig. 3 Effects of sequestered TGF-β3 on chondrogenic differentiation by hASCs and their underlying mechanism. a Immunofluorescence staining of accumulated chondroitin sulfate and type II collagen in hydrogels. Scale bar: 300 μm. **b** Chondrogenic gene expression from hASCs cultured in the indicated hydrogels. **c** Extracellular matrix analysis. sGAG contents (left) and collagen contents (right). **d** TGF-β ligand gene expression. **e** CD44 gene expression in hASCs cultured in the indicated hydrogels. **f** Signaling pathway-related protein expression in hASCs cultured in the indicated hydrogels. ($n = 3$; $^{*}P < 0.05$, $^{**}P < 0.01$, $^{***}P < 0.001$ vs. HA; $^{\#}P < 0.05$, $^{\#\#}P < 0.01$, $^{\#\#\#}P < 0.001$ vs. Sol-T).

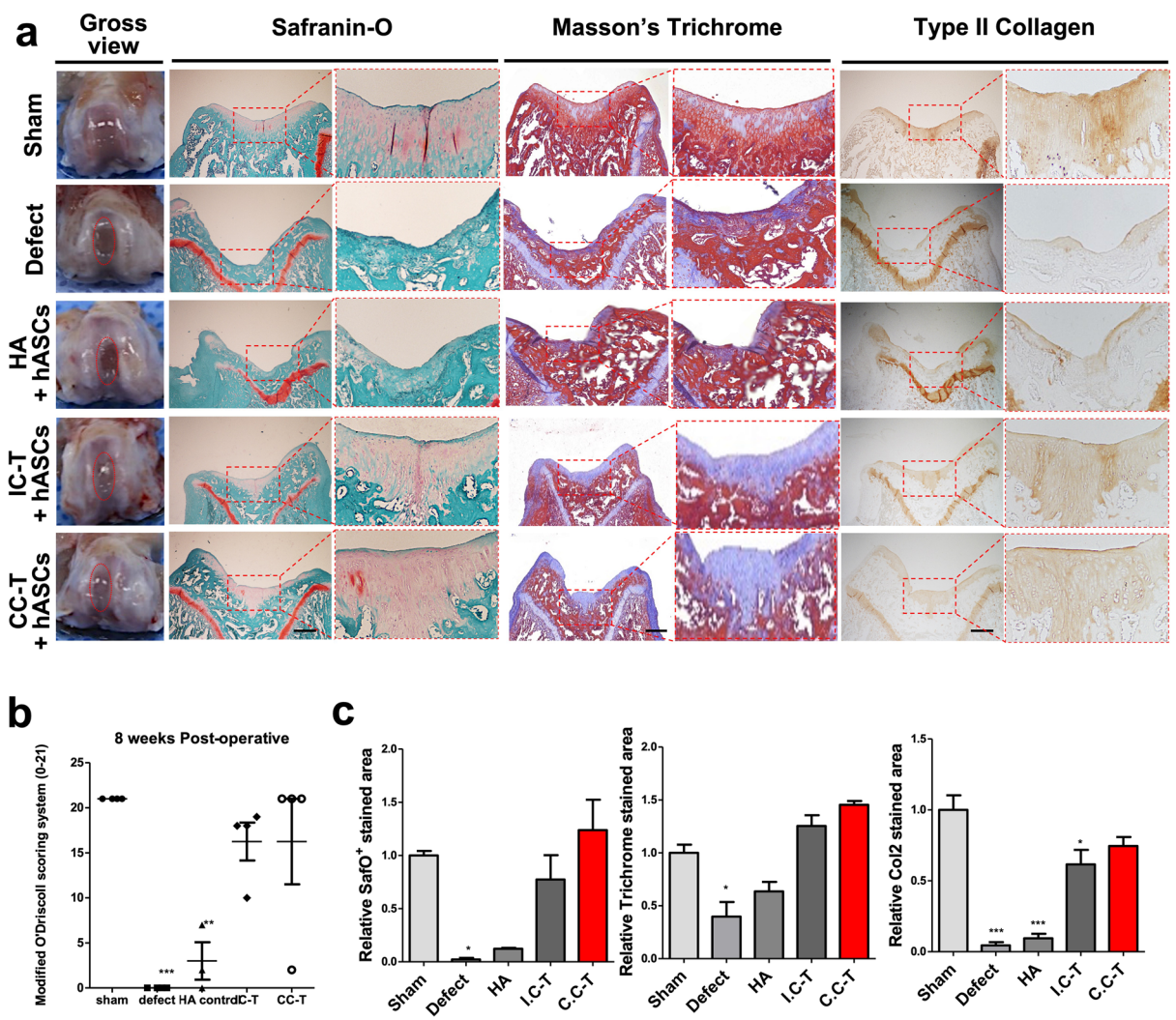

Fig. 4 Representative macroscopic observation and histological evaluation of repaired tissue 8 weeks after surgery. a Gross appearance, Safranin O staining, Masson's trichrome staining, and immunohistochemistry staining of the repaired cartilage defects. Red dashed circles indicate cartilage defect areas. Scale bar: 500 μm. **b** O'Driscoll scores of the repaired tissue 8 weeks after surgery. **c** left to right: Safranin O, trichrome, and type II collagen-stained area. ($n = 4$; *$P < 0.05$, ***$P < 0.001$ vs. sham).

filling, a rough surface, and low levels of Safranin O, total collagen, and type II collagen staining relative to the neighboring native cartilage. In contrast, the hASC+IC-T and hASC+CC-T groups exhibited complete defect filling, with tissue that more closely resembled the neighboring native cartilage in structure, and higher intensity of staining for Safranin O, total collagen, and type II collagen staining. In addition, defect healing in the hASC +IC-T and hASC+CC-T groups was associated with lower expression of hypertrophic markers and type I collagen (Fig. S3, Supporting Information). Quantitative evaluation of the quality of cartilage tissue regeneration using the modified O'Driscoll histologic scoring system revealed a significantly improved histologic score in the IC-T and CC-T groups, comparable to that in native cartilage (sham) ($p > 0.05$). Similarly, previous studies reported that TGF-tethered hydrogel systems, such as TGF-β1-sequestered visible blue light crosslinkable chitosan hydrogels[53] and TGF-β1-sequestered UV crosslinkable PEG hydrogels[17,65], can promote chondrogenesis of MSCs or chondrocytes in vitro and/or in vivo. These data suggest that both IC-T and CC-T systems, which sequester TGF-β3 in distinct ways, are efficient methods for improving cartilage regeneration. In animal studies, the CC-T group exhibited the regenerative effect most similar to that of the sham group and was also most similar in terms of Safranin O, immunofluorescence, and Masson's trichrome staining.

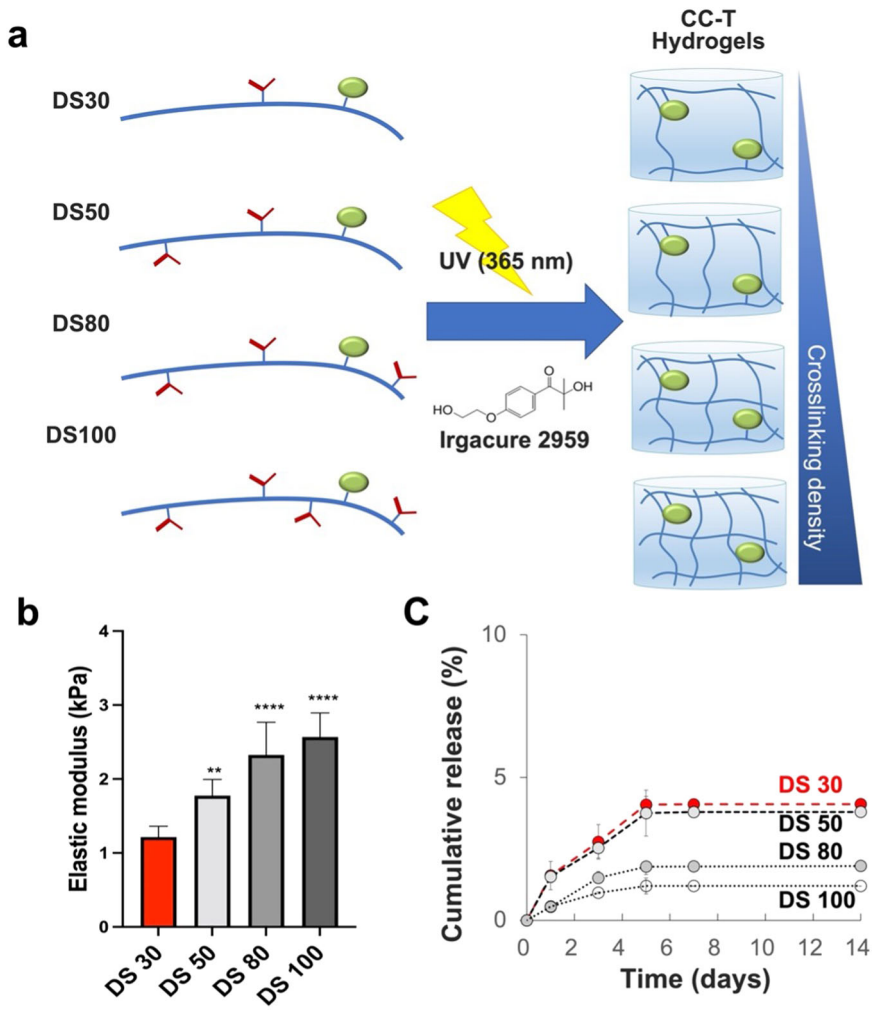

Fig. 5 Preparation of CC-T with different mechanical properties. a Schematic representation of the experimental groups. **b** Mechanical characterization of hydrogels. **c** TGF-β3 release profile in the indicated CC-T hydrogels. ($n = 4$; *$P < 0.05$, **$P < 0.01$, ***$P < 0.001$ vs. DS30).

Biochemical plus biophysical effects on chondrogenic differentiation in the 3D environment of the HA hydrogel

To determine the effects of physical cues on the 3D chondrogenesis signaling pathways, we varied the DS of MAHA from 30 to 100 (Figure S4, Supporting Information) by varying the feed ratio of methacrylic anhydride (Fig. 5a). The elastic modulus of the hydrogel increased as the DS of MAHA increased: 1.0 kPa, 1.6 kPa, 2.1 kPa, and 2.5 kPa for DS30, 50, 80, and 100, respectively (Fig. 5b). Among the two TGF-β3 sequestering systems, CC-T was more suitable for observing the effect of physical factors because it changed only the elastic modulus of the hydrogels during the experiment while maintaining the content of the chemical factor TGF-β3; CC-T retained more than 95% of TGF-β3 in all groups (Fig. 5c, S5, Supporting Information).

After 2 weeks of induction of chondrogenesis in the hASCs encapsulated in each hydrogel, chondrogenic gene expression was significantly higher in DS30, whereas osteogenic and hypertrophic gene expression was significantly lower in DS30 (Fig. 6a). Chondroitin sulfate and type II collagen expression were also significantly higher in DS30 (Fig. 6b). The quantitative evaluation revealed that sGAG and collagen content decreased as a function of DS (Fig. 6c), indicating that chondrogenesis by encapsulated hASCs was highly increased in soft hydrogels.

To elucidate 3D signaling during chondrogenesis, we first evaluated the levels of CD44 and ALK5 in the hASCs encapsulated in hydrogels. Interestingly, although we used the same concentration [0.5% (w/v)] of HA and TGF-β3 for all hydrogels (DS30, 50, 80, and 100), the hASCs encapsulated in soft hydrogel (DS30) expressed significantly higher levels of CD44 and ALK5 than in more substituted, harder hydrogels. The *CD44* mRNA level was well correlated with protein expression (Fig. S6,

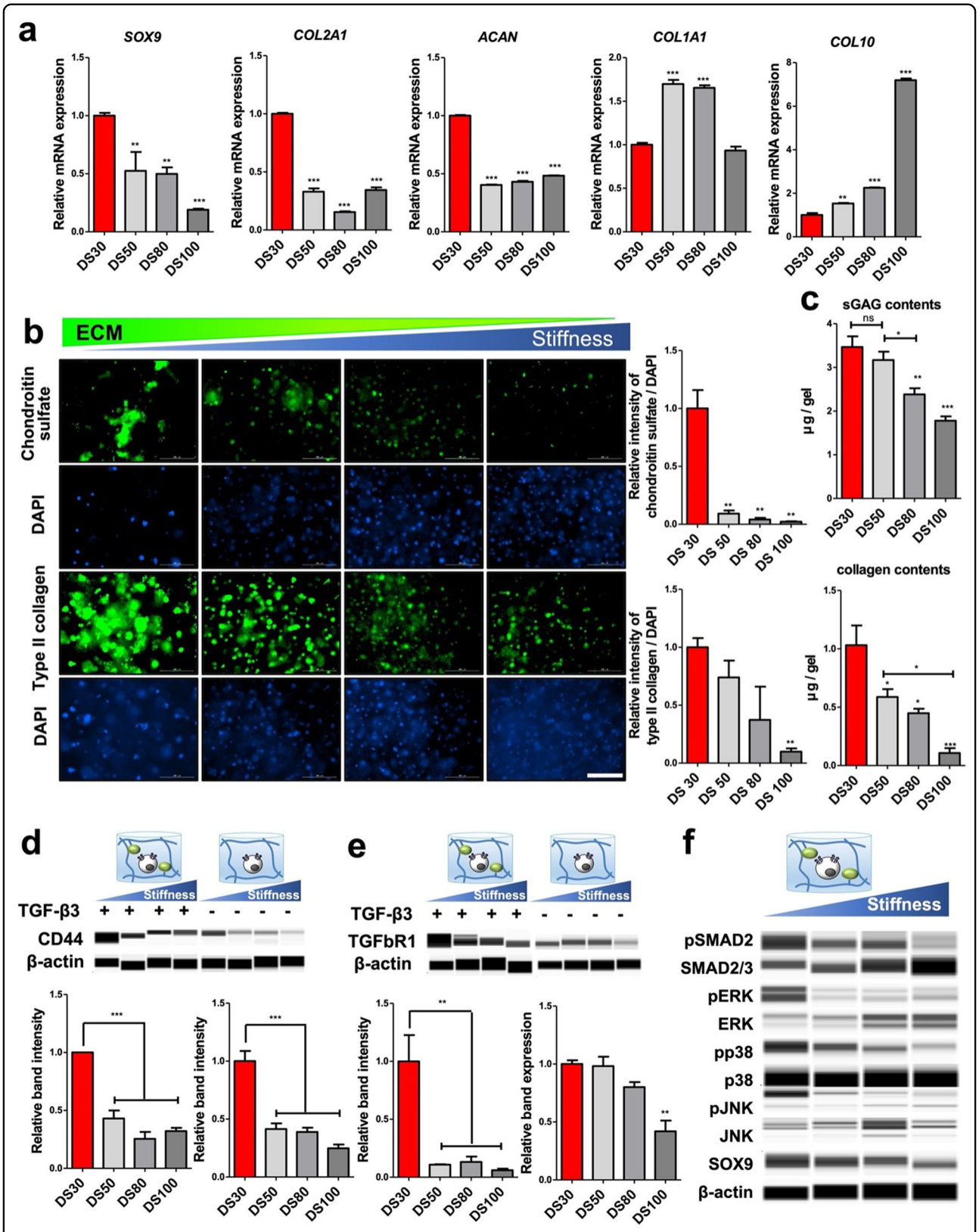

Fig. 6 Effect of microenvironmental stiffness on signal transduction. a Chondrogenic and hypertrophic gene expression. **b** Immunofluorescence staining of accumulated chondroitin sulfate and type II collagen in hydrogels. Scale bar: 300 μm. **c** sGAG and collagen contents. **d** CD44 and **e** ALK5 expression. **f** Signaling pathway-related protein expression. ($n = 3$; $^{*}P < 0.05$, $^{**}P < 0.01$, $^{***}P < 0.001$ vs. DS30).

Supporting Information). Interestingly, the expression of CD44 and ALK5 was lower in the hASCs encapsulated in the hydrogels without TGF-β3 than in those encapsulated in DS100 with TGF-β3 (Fig. 6d, e). Park et al. also reported that TGF-β increased chondrogenic marker expression, such as type II collagen, in MSCs on soft substrates but not on stiff substrates. However, they investigated this differential effect on a 2D environment[51]. In our findings, the physicochemical cues in the 3D cellular microenvironment also suggest that the elevated expression of CD44 and ALK5 in the hASCs encapsulated in the soft DS30 hydrogel could be attributed to the synergistic effect of the TGF-β3-conjugated HA backbone in the less crosslinked DS30 hydrogel, which would presumably promote interaction with receptors on the encapsulated hASCs. Therefore, the synergistic crosstalk between CD44 and ALK5 induced an increase in the chondrogenesis of hASCs in the HA hydrogel. Bourguignon et al. reported that ALK5 contains a CD44-binding site and that binding of HA to CD44 stimulates ALK5 activity, thereby increasing Smad2/3 phosphorylation[66]. In addition, the elevated CD44 and ALK5 expression in the hASCs encapsulated in DS30 hydrogels promoted phosphorylation of SMAD2, ERK, p38, and JNK (Fig. 6f). Through these mechanisms, the expression of SOX9 was also increased in the hASCs encapsulated in DS30, and the accumulation of chondroitin sulfate and type II collagen was further elevated.

Combinatorial ultrasonic stimulation effects chondrogenic differentiation in the 3D environment of the HA hydrogel

We studied the synergistic effect of sequestered TGF-β3 and external stimulation on 3D chondrogenic signaling pathways. For external stimulation, we used US, which has a positive effect on chondrogenesis and cartilage repair[67–69]. First, we characterized the relationship between US stimulation time and cytotoxicity (Fig. S7a, Supporting Information). The optimal stimulation time was determined based on the level of type II collagen (Fig. S7b, Supporting Information). The cells were incubated for 14 days, with replacement of the medium every 2 days. At the time of the medium change, a US impulse was applied from the bottom of the tube containing the hydrogel-encapsulated hASCs and medium (Fig. 7a, b). Immunofluorescence staining for accumulated chondroitin sulfate and type II collagen revealed that the expression of chondrogenic markers was significantly higher in CC-T with US (CC-T + US) than in HA, HA with US (HA + US), and CC-T (Fig. 7c). qRT-PCR revealed that US stimulation increased the expression of *SOX9*, *ACAN*, and *COL2A1* (Fig. 7d). In addition, US stimulation increased the ECM content (Fig. S8, Supporting Information).

To understand the mechanisms underlying these changes, we analyzed TGF ligands. After external US stimulation was applied to the HA and CC systems, the level of *CD44* mRNA in the encapsulated hASCs was significantly elevated (Fig. 7e). This result may be due to the movement of the HA backbone induced by US stimulation, which increases the chance of interaction between the CD44 binding site in HA with cells encapsulated in the HA and CC hydrogels[66]. Based on these results, we propose the existence of a signaling pathway activated by US stimulation in HA hydrogel that promotes the expression of CD44, ALK5, and pERK (Fig. 7f).

In summary, we developed an advanced comprehensive 3D environment with photocrosslinked HA that enabled us to characterize the combinatorial effects of dimensionality, localization of chemical cues, regulation of physical cues, and external stimulation on the chondrogenic signaling pathways in hASCs. The combination of TGF chemical conjugation (biochemical cue) and soft modulus (biophysical cue) in 3D hydrogels under ultrasound stimulation could indeed amplify chondrogenesis. Therefore, our findings have important ramifications for cartilage regeneration and regenerative medicine applications.

Materials and methods

Preparation of photocrosslinkable hyaluronic acid

MAHA with a degree of substitution of DS50 was synthesized as previously reported[70]. Briefly, methacrylic anhydride (8 mL, Sigma-Aldrich, St. Louis, MO) was added to a 1% w/v HA (Mw 500 kDa, Bioland, Korea) aqueous solution. The mixture was allowed to react for 24 h with stirring at 4 °C after the pH was adjusted to 8.0 using 5 N NaOH solution. The reaction mixture was dialyzed against deionized water for 3 days using a membrane with a cutoff molecular weight of 100 kDa, followed by lyophilization. The DS was calculated from the relative peak integration ratios of the methacrylate protons (peaks at ~6.1, 5.6, and 1.85 ppm) and methyl protons of HA (~1.9 ppm). The DS of the final product was confirmed to be 50% by ^{1}H-NMR. DS30, DS80, and DS100 were similarly prepared by regulating the amount of methacrylic anhydride and 5 N NaOH.

Preparation of HA hydrogels

For the preparation of HA hydrogels, MAHA polymer solution (0.5% w/v) in phosphate-buffered saline (PBS) was prepared with a photoinitiator, Irgacure 2959 (final concentration 0.2% w/v). For creation of a polydimethylsiloxane (PDMS) mold, 40 μl of polymer solution was added with a depth of 2 mm and a diameter of 5 mm and then exposed to UV light (365 nm, 60 mW/cm^2, Sei Myung Vactron Co., Ltd., Korea) for 10 sec.

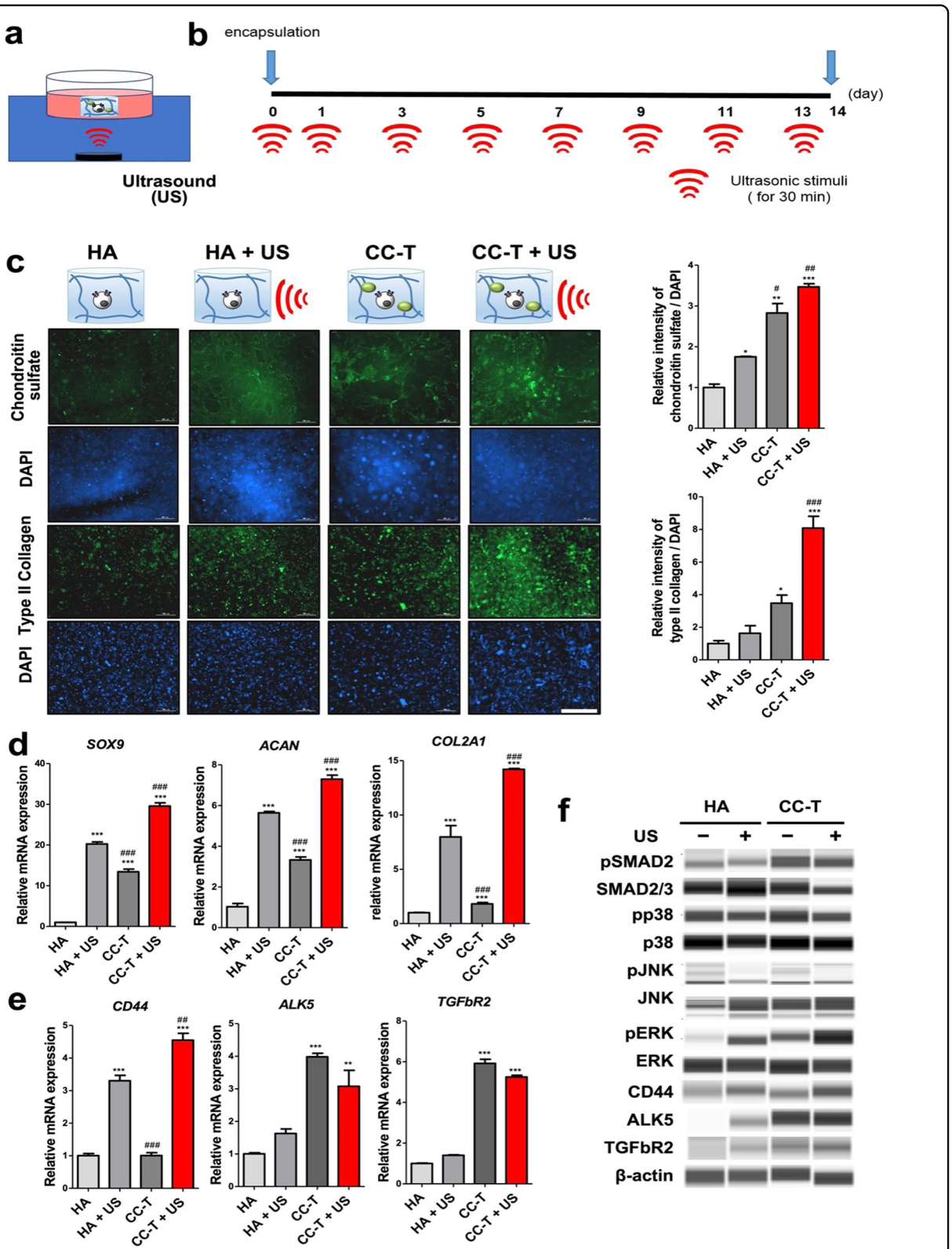

Fig. 7 Synergistic effect of sequestered TGF-β3 and external stimulation. a Schematic representation of the delivery of ultrasound (US) stimulus to HA hydrogel. **b** Schedule for US stimuli. **c** Immunofluorescence staining of accumulated chondroitin sulfate and type II collagen in HA and CC hydrogels. **d** Chondrogenic gene expression. **e** TGF ligand gene expression. **f** Signaling pathway-related protein expression. ($n = 3$; $^{*}P < 0.05$, $^{**}P < 0.01$, $^{***}P < 0.001$ vs. HA; $^{\#}P < 0.05$, $^{\#\#}P < 0.01$, $^{\#\#\#}P < 0.001$ vs. HA + US).

Conjugation of TGF-β3 with methacrylated hyaluronic acid

TGF-β3-conjugated MAHA was prepared by ionic (IC-T) or covalent conjugation (CC-T). The attraction between the positively charged regions in TGF-β3 and the negatively charged carboxyl groups in MAHA induces ionic bonds. For IC-T, TGF-β3 was mixed and reacted with MAHA solution at a final TGF-β3 concentration of 2 μg/ml for 2 h at 37 °C. For CC-T, carboxyl groups of MAHA were activated as NHS ester using 1-ethyl-3-(3-dimethylanimopropyl) carbodiimide (EDC)/N-hydroxysulfosuccinimide sodium salt (NHS) in 50 mM 2-(N-morpholino) ethanesulfonic acid (MES) buffer (pH 6) for 2 h at room temperature and subsequently reacted with amine groups of TGF-β3 in PBS. Briefly, 2 μg of TGF-β3 was added and reacted overnight at 4 °C and purified using a 100 kDa Amicon Ultra-0.5 centrifugal filter (Millipore UFC510024). The calculated conversion rate was 99%.

Mechanical characterization of hydrogels

We performed the same experiment described in our previous paper[47]. Briefly, we used a customized bulk-scale nanoindenter consisting of a load cell (GS0-10, Transducer Techniques) and an automated stage (SM2-0803-3S and SZ-0604-3S, ST1) equipped with a microscope (AM4113, AnMo Electronics Corporation) to characterize the mechanical characteristics of hydrogels with various degrees of stiffness. A stainless spherical tip with a 2 mm diameter was attached to the load cell for indentation. The contact between the tip and the hydrogel was assumed to be Hertzian. The maximum indentation depth was ~5% of the hydrogel thickness, and the indentation speed was 25 μm/s. Both the applied force and the indentation depth were recorded at an acquisition rate of 10 Hz during the experiment. The effective modulus of the hydrogel was estimated by fitting a force-indentation curve to the Hertzian model given by Eq. (1):

$$F = \frac{4}{3} \cdot \frac{E}{1-\nu^2} \cdot \sqrt{r} \cdot \delta^{\frac{3}{2}} \quad (1)$$

where F is the applied force, E is Young's modulus of the hydrogel, ν is the Poisson's ratio of the hydrogel, which is assumed to be 0.5, r is the radius of the indentation tip, and δ is the indentation depth.

hASC isolation

Human adipose-derived stem cells were isolated from adipose tissues around the patients' knee with the approval of the Ethics committee at CHA University (IRB No. 2014-07-096). In brief, adipose tissues were washed with PBS containing 2% penicillin/streptomycin (P/S) and digested by chopping after 0.5 mg/ml collagenase type II (Sigma-Aldrich, St. Louis, MO) treatment for 45 min at 37 °C in an incubator shaker. Digested tissues were filtered through a 40 μm pore size cell strainer. The filtered tissue solution was washed three times with Dulbecco's modified Eagle's medium (DMEM; HyClone, Logan, UT) by centrifugation at 1000 × *g* for 10 min. The cell pellet was resuspended in DMEM with 20% v/v fetal bovine serum (FBS) and 1% v/v P/S. The cells were cultured on tissue culture plates at 37 °C in a 5% CO_2 incubator. The culture medium was changed every 3 days.

hASC 2D culture and 3D culture

The hASCs were cultured in DMEM low glucose media (HyClone, USA) with 10% fetal bovine serum (FBS, HyClone, USA) and 1% penicillin/streptomycin (P/S, HyClone, USA) at 37 °C in a 5% CO_2 incubator. For 3D culture, MAHA polymer solution (0.5% w/v) in PBS was prepared with a photoinitiator, Irgacure 2959 (final concentration 0.2% w/v). Then, hASCs (passage 3) were encapsulated at a density of 5×10^6 cells/mL. Each hydrogel was cultured under media conditions of 1 ml and 1 gel per well of a 24-well plate. For chondrogenic differentiation, the medium conditions were DMEM high glucose media (HyClone, USA) with 10% FBS, 1% P/S, insulin-transferrin-selenium (ITS), 10 μg/ml transforming growth factor beta 3 and 100 nM dexamethasone.

qRT-PCR

For qRT-PCR analysis, HA hydrogel was collected after 14 days of chondrogenic induction culture. The HA hydrogel was frozen with liquid nitrogen and broken with a homogenizer in 200 μl of TRIzol TM (Life Technologies, USA). After the hydrogel was broken, 800 μl of TRIzol and 200 μl of chloroform were added. After inverting the sample five times and centrifuging at 13,000 rpm and 4 °C for 20 min, we mixed the supernatant with the same volume of isopropanol. The mixture was centrifuged at 13,000 rpm and 4 °C for 20 min and washed with 70% ethanol. After another centrifugation at 13,000 rpm and 4 °C for 10 min, the pellet was dried and weighed for quantification. For cDNA synthesis, the TaKaRa cDNA synthesis kit (TaKaRa, Japan) was used, and quantitative real-time PCR was performed using Power SYBR® Green PCR Master Mix (Applied Biosystems, UK). As a housekeeping gene, the ribosomal protein S18 (*RPS18*) gene was used to standardize gene expression for real-time PCR analysis. Primers for SRY-related HMG-box9 (*SOX9*), aggrecan (*ACAN*), type II collagen (*COL2A1*), type I collagen (*COL1A1*), type X collagen (COL10), TGF receptor 1 *(ALK5)*, TGF receptor 2 (*TGFbR2*), and CD44 were used. The PCR primer sequences are shown in Table S1, Supporting Data.

Western blot (or simple western, WES)

Western blotting was performed using WES according to the manufacturer's protocol (Protein Simple, San Jose,

CA, USA). In detail, HA hydrogel was collected after 1 h of chondrogenic induction culture. The hydrogel was washed three times with PBS and frozen with liquid nitrogen. Then, the hydrogel was lysed with a homogenizer in 50 µl of 5X RIPA buffer. The supernatant was collected. The protein concentration was measured with a bicinchoninic acid protein assay. The prepared protein samples, blocking reagent, primary antibodies, secondary antibodies, chemiluminescent substrate, and wash buffer were added to the assay plate. The plate was placed in the instrument, and protein separation and detection were performed automatically. For the primary antibodies, anti-chondroitin sulfate antibody (Abcam ab11570), Sox9 (D8G8H) 82630S, anti-collagen type II antibody (MAB8887), anti-beta-actin (Abm G043), anti-phospho-SAPK/JNK (Thr183/Tyr185) (CST 4668S), anti-JNK2 (56G8) (CST 9258S), anti-phospho-p44/42 MAPK (Erk1/2) (CST 4377S), anti-p44/42 MAPK (CST 9102S), anti-phospho-p38 MAPK (CST 4613S), anti-phospho-MEK1/2 (CST 9121S), anti-phospho-Smad2 (CST 3108S), and anti-SMAD2/3 (CST 3102S) were used with anti-mouse or anti-rabbit secondary antibodies provided by ProteinSimple.

Immunofluorescence staining

After 14 days of induction of chondrogenic differentiation, the HA hydrogel was washed three times with Dulbecco's phosphate-buffered saline (DPBS), and the washed gel was fixed overnight at 4 °C with 4% paraformaldehyde (Biosesang, Korea). The fixed gel was permeabilized with 0.3% Triton X-100 in DPBS (PBS-T), and the hydrogel was blocked with 1% bovine serum albumin (BSA)-PBST for 1 h at room temperature. The primary antibody was diluted 1:100 in 1% BSA-PBST solution, and the hydrogels were incubated in the primary antibody solution at 4 °C for 24 h. Fluorescein-conjugated secondary antibodies (Alexa Fluor 488 goat anti-mouse IgG (H + L)) and Texas Red goat anti-rabbit IgG (H + L) (Life Technologies) were diluted at a ratio of 1:500 and incubated at room temperature for 2 h. The cells were stained with 4'6-diamidino-2-phenylindole to identify the nuclei and observed with a fluorescence microscope.

sGAG analysis

Sulfated-glycosaminoglycan (sGAG) was measured using a Blyscan sulfated glycosaminoglycan assay kit (Biocolor B1000) after 14 days of chondrogenesis. The sGAG assay was performed according to the manufacturer's protocol. In brief, 10 µl of each hydrogel was adjusted to 100 µl with deionized water or the appropriate buffer. Blyscan dye reagent (1.0 ml) was added to each tube, mixed by inverting the contents and placed in a gentle mechanical shaker for 30 min. The tubes were transferred to a microcentrifuge and spun at 12,000 rpm for 10 min. A dissociation reagent (0.5 ml) was then added to the tubes. When all of the bound dye was dissolved, the tubes were centrifuged at 12,000 rpm for 5 min to remove excess foam. Afterward, 200 µl of each sample was transferred to individual wells of a 96-well microplate. The microplate reader was set to 656 nm or the closest matching red filter.

Collagen analysis

Collagen content was measured using a hydroxyproline assay kit (Gibco MAK008). Collagen was analyzed according to the manufacturer's protocol. First, 10 mg of the hydrogel cultured for 14 days in chondrogenic medium was homogenized in 100 µl of water and transferred to a capped tube. Afterward, 100 µl of concentrate was hydrolyzed at 120 °C for 3 h. The solution was mixed and centrifuged at $10{,}000 \times g$ for 3 min, and 10 µl of the supernatant was transferred to a 96-well plate. The wells were evaporated in a 60 °C oven to dry the samples, and 100 µl of Chloramine T/Oxidation Buffer Mixture was added to each sample and standard well. The plate was incubated at room temperature for 5 min. Afterward, 100 µl of diluted para-dimethylaminobenzaldehyde reagent was added to each sample and standard well and incubated for 90 min at 60 °C. The absorbance was measured at 560 nm (A_{560}).

In vivo study

The experimental protocol for animal surgery was performed in accordance with the protocols approved by the CHA University Institutional Animal Care and Use Committee guidelines for the care and use of laboratory animals (Approval number # IACUC160052). Male Sprague-Dawley (SD) rats (10–12 weeks old, 300–350 g; Orient Bio, Inc., Seongnam, Korea) were used; four rats in the sham group and five rats in each group were used. Animals were anesthetized with a mixture of Zoletil (50 mg/kg; Virbac Laboratories, Carros, France) and Rompun (10 mg/kg; Bayer, Seoul, South Korea). Knee joint areas were shaved and disinfected. A medical parapatellar longitudinal incision was performed to crop out the synovial capsule on the knee joint, and the trochlear groove was removed after lateral patellar luxation. A hole with a diameter of 2 mm and a depth of 2 mm was made by drilling through the center of the trochlear groove. Hyaluronic acid hydrogel was directly added to the hole. For each defect site, 3 µl of MAHA solution and 15,000 cells were used. After a total of 8 weeks, the SD rats were sacrificed, and the results of the animal experiments were analyzed using paraffin blocks. We performed Safranin O staining to confirm cartilage regeneration and assessed type II collagen using immunohistochemistry to identify hyaline cartilage.

Ultrasound stimulation

The ultrasound was generated by a Nanosonic instrument (Korust, Korea). Ultrasound was transmitted through a transducer placed in a water tank. Ultrasonic stimulation was applied for 30 min at a frequency of 1 MHz and an intensity of 300 mW/cm^2. Ultrasonic stimulation was applied once every 2 days, and a medium change was performed directly after stimulation.

Statistical analysis

Statistical analysis of the results was performed using GraphPad Prism ver. 8.0 (GraphPad software, San Diego, CA). One-way ANOVA using Tukey's multiple comparison post-test was performed to compare the samples. Statistical significance was set at $^{*}P < 0.05$, $^{**}P < 0.01$, and $^{***}P < 0.001$ and $^{\#}P < 0.05$, $^{\#\#}P < 0.01$, and $^{\#\#\#}P < 0.001$.

Acknowledgements

This work was supported by the National Research Foundation of Korea (NRF) grants funded by the Korean government (MSIT and MOE) (NRF-2022R1A2C3004850, NRF-2019M3A9H1032376, and NRF-2020R1IA1A01074331) and a grant of the Korea Health Technology R&D Project through the Korea Health Industry Development Institute (KHIDI), funded by the Ministry of Health & Welfare, Republic of Korea (HI19C0757) and the Korean Fund for Regenerative Medicine (KFRM) grant funded by the Korean government (the Ministry of Science and ICT, the Ministry of Health & Welfare) (21C0703L1).

Author details

[1]Department of Medical Biotechnology, Dongguk University, 32 Dongguk-ro, Ilsandong-gu, Goyang, Gyeonggi 10326, Republic of Korea. [2]Department of Pharmaceutical Sciences, Department of Biomedical Engineering & Biointerfaces Institute, University of Michigan, Ann Arbor, MI 48109, USA. [3]Department of Neurosurgery, Yonsei University College of Medicine, 50 Yonsei-ro, Seodaemun-gu, Seoul 120-752, Republic of Korea. [4]Department of Biomedical Science, CHA University, 335 Pangyo-ro, Bundang-gu, Seongnam-si, Gyeonggi-do 13488, Republic of Korea

Author contributions

S.-H.L. and J.A. conceptualized and designed this study. J.A. and Y.A. carried out the experiments and generated the data. B.J.K. supported the in vivo study. All authors contributed to the final version of the manuscript. Y.-K.S., J.J.M., D.A.S., B.C., and S.-H.L. elaborately reviewed and revised the manuscript. The entire study was conducted under the supervision of S.-H.L.

Competing interests

The authors declare no competing interests.

Supplementary information The online version contains supplementary material available at https://doi.org/10.1038/s41427-022-00387-3.

Received: 3 November 2021 Revised: 7 March 2022 Accepted: 31 March 2022.
Published online: 3 June 2022

References

1. Cukierman, E., Pankov, R. & Yamada, K. M. Cell interactions with three-dimensional matrices. *Curr. Opin. Cell Biol.* **14**, 633–639 (2002).
2. Alessio, N. et al. Timely supplementation of hydrogels containing sulfated or unsulfated chondroitin and hyaluronic acid affects mesenchymal stromal cells commitment toward chondrogenic differentiation. *Front. Cell Dev. Biol.* **9**, 641529 (2021).
3. Vining, K. H. & Mooney, D. J. Mechanical forces direct stem cell behaviour in development and regeneration. *Nat. Rev. Mol. Cell Biol.* **18**, 728–742 (2017).
4. Blaber, E. A. et al. Mechanical unloading of bone in microgravity reduces mesenchymal and hematopoietic stem cell-mediated tissue regeneration. *Stem Cell Res.* **13**, 181–201 (2014).
5. Jeon, O. et al. Mechanical properties and degradation behaviors of hyaluronic acid hydrogels cross-linked at various cross-linking densities. *Carbohydr. Polym.* **70**, 251–257 (2007).
6. Nava, M. M., Raimondi, M. T. & Pietrabissa, R. Controlling self-renewal and differentiation of stem cells via mechanical cues. *J. Biomed. Biotechnol.* **2012**, 797410 (2012).
7. Schaffer, A. C. A. D. V. Biophysical regulation of stem cell behavior within the niche. *Stem Cell Res. Therapy* **3**, 50 (2012).
8. Kulangara, K., Yang, Y., Yang, J. & Leong, K. W. Nanotopography as modulator of human mesenchymal stem cell function. *Biomaterials* **33**, 4998–5003 (2012).
9. Yang, Y., Wang, K., Gu, X. & Leong, K. W. Biophysical regulation of cell behavior—cross talk between substrate stiffness and nanotopography. *Engineering* **3**, 36–54 (2017).
10. Tsou, Y. H., Khoneisser, J., Huang, P. C. & Xu, X. Hydrogel as a bioactive material to regulate stem cell fate. *Bioact. Mater.* **1**, 39–55 (2016).
11. Huang, Q. et al. Hydrogel scaffolds for differentiation of adipose-derived stem cells. *Chem. Soc. Rev.* **46**, 6255–6275 (2017).
12. Bian, L. et al. The influence of hyaluronic acid hydrogel crosslinking density and macromolecular diffusivity on human MSC chondrogenesis and hypertrophy. *Biomaterials* **34**, 413–421 (2013).
13. Cui, J. H., Park, K., Park, S. R. & Min, B.-H. Effects of low-intensity ultrasound on chondrogenic differentiation of mesenchymal stem cells embedded in polyglycolic acid- an in vivo study. *Tissue Eng.* **12**, 75–82 (2006).
14. Kim, J. et al. TGF-β1 conjugated chitosan collagen hydrogels induce chondrogenic differentiation of human synovium-derived stem cells. *J. Biol. Eng.* **9**, https://doi.org/10.1186/1754-1611-9-1 (2015).
15. Masters, K. S. Covalent growth factor immobilization strategies for tissue repair and regeneration. *Macromol. Biosci.* **11**, 1149–1163 (2011).
16. Mitchell, A. C., Briquez, P. S., Hubbell, J. A. & Cochran, J. R. Engineering growth factors for regenerative medicine applications. *Acta Biomaterialia* **30**, 1–12 (2016).
17. Sridhar, B. V., Doyle, N. R., Randolph, M. A. & Anseth, K. S. Covalently tethered TGF-beta1 with encapsulated chondrocytes in a PEG hydrogel system enhances extracellular matrix production. *J. Biomed. Mater. Res. A* **102**, 4464–4472 (2014).
18. Ito, T., Sawada, R., Fujiwara, Y. & Tsuchiya, T. FGF-2 increases osteogenic and chondrogenic differentiation potentials of human mesenchymal stem cells by inactivation of TGF-β signaling. *Cytotechnology* **56**, 1–7 (2007).
19. Leslie-Barbick, J. E., Moon, J. J. & West, J. L. Covalently-immobilized vascular endothelial growth factor promotes endothelial cell tubulogenesis in poly (ethylene glycol) diacrylate hydrogels. *J. Biomater. Sci., Polym. Ed.* **20**, 1763–1779 (2009).
20. Shen, Y. H., Shoichet, M. S. & Radisic, M. Vascular endothelial growth factor immobilized in collagen scaffold promotes penetration and proliferation of endothelial cells. *Acta Biomater.* **4**, 477–489 (2008).
21. Li, H. et al. A hydrogel bridge incorporating immobilized growth factors and neural stem/progenitor cells to treat spinal cord injury. *Adv. Health. Mater.* **5**, 802–812 (2016).
22. Ragothaman, M., Palanisamy, T. & Kalirajan, C. Collagen-poly(dialdehyde) guar gum based porous 3D scaffolds immobilized with growth factor for tissue engineering applications. *Carbohydr. Polym.* **114**, 399–406 (2014).
23. Madry, H., Rey-Rico, A., Venkatesan, J. K., Johnstone, B. & Cucchiarini, M. Transforming growth factor beta-releasing scaffolds for cartilage tissue engineering. *Tissue Eng. Part B Rev.* **20**, 106–125 (2014).
24. Yin, F. et al. Cartilage regeneration of adipose-derived stem cells in the TGF-beta1-Immobilized PLGA-gelatin scaffold. *Stem Cell Rev. Rep.* **11**, 453–459 (2015).
25. Dünker, N. & Krieglstein, K. Targeted mutations of transforming growth factor-β genes reveal important roles in mouse development and adult homeostasis. *Eur. J. Biochem.* **267**, https://doi.org/10.1046/j.1432-1327.2000.01825.x (2001).
26. Grimaud, E., Heymann, D. & Rédini, F. Recent advances in TGF-β effects on chondrocyte metabolism: Potential therapeutic roles of TGF-β in cartilage

disorders. *Cytokine Growth Factor Rev.* **13**, https://doi.org/10.1016/S1359-6101(02)00004-7 (2002).
27. Tang, Q. O. et al. TGF-β3: a potential biological therapy for enhancing chondrogenesis. *Expert Opin. Biol. Therapy* **9**, https://doi.org/10.1517/14712590902936823 (2009).
28. Schiffer, M., Von Gersdorff, G., Bitzer, M., Susztak, K. & Böttinger, E. P. Smad proteins and transforming growth factor-β signaling. *Kidney Int.* **58**, S45–S52 (2000).
29. Pivetta, E. et al. Blood-derived human osteoclast resorption activity is impaired by Hyaluronan-CD44 engagement via a p38-dependent mechanism. *J. Cell Physiol.* **226**, 769–779 (2011).
30. Coricor, G. & Serra, R. TGF-beta regulates phosphorylation and stabilization of Sox9 protein in chondrocytes through p38 and Smad dependent mechanisms. *Sci. Rep.* **6**, 38616 (2016).
31. Choi, J. H. et al. Evaluation of hyaluronic acid/agarose hydrogel for cartilage tissue engineering biomaterial. *Macromol. Res.* **28**, 979–985 (2020).
32. Wu, Y. et al. The combined effect of substrate stiffness and surface topography on chondrogenic differentiation of mesenchymal stem cells. *Tissue Eng. Part A* **23**, 43–54 (2017).
33. Allen, J. L., Cooke, M. E. & Alliston, T. ECM stiffness primes the TGFbeta pathway to promote chondrocyte differentiation. *Mol. Biol. Cell* **23**, 3731–3742 (2012).
34. Razinia, Z. et al. Stiffness-dependent motility and proliferation uncoupled by deletion of CD44. *Sci. Rep.* **7**, 16499 (2017).
35. Kim, Y. & Kumar, S. CD44-mediated adhesion to hyaluronic acid contributes to mechanosensing and invasive motility. *Mol. Cancer Res.* **12**, 1416–1429 (2014).
36. Srinivasan, A., Chang, S. Y., Zhang, S., Toh, W. S. & Toh, Y. C. Substrate stiffness modulates the multipotency of human neural crest derived ectomesenchymal stem cells via CD44 mediated PDGFR signaling. *Biomaterials* **167**, 153–167 (2018).
37. Mouw, J. K., Connelly, J. T., Wilson, C. G., Michael, K. E. & Levenston, M. E. Dynamic compression regulates the expression and synthesis of chondrocyte-specific matrix molecules in bone marrow stromal cells. *Stem Cells* **25**, 655–663 (2007).
38. Esfandiari, E. et al. Induction of chondrogenic differentiation of human adipose-derived stem cells by low frequency electric field. *Adv. Biomed. Res.* **5**, https://doi.org/10.4103/2277-9175.183146 (2016).
39. Hanifi, A. et al. Near infrared spectroscopic assessment of developing engineered tissues: correlations with compositional and mechanical properties. *Analyst* **142**, 1320–1332 (2017).
40. Elder, B. D. & Athanasiou, K. A. Hydrostatic pressure in articular cartilage tissue engineering: from chondrocytes to tissue regeneration. *Tissue Eng. Part B, Rev.* **15**, https://doi.org/10.1089/ten.teb.2008.0435 (2009).
41. Yousefi, F., Kim, M., Nahri, S. Y., Mauck, R. L. & Pleshko, N. Near-infrared spectroscopy predicts compositional and mechanical properties of hyaluronic acid-based engineered cartilage constructs. *Tissue Eng. Part A* **24**, https://doi.org/10.1089/ten.tea.2017.0035 (2018)
42. Loyola-Sánchez, A. M. et al. Effect of low-intensity pulsed ultrasound on the cartilage repair in people with mild to moderate knee osteoarthritis: a double-blinded, randomized, placebo-controlled pilot study. *Arch. Phys. Med. Rehabilitation* **93**, https://doi.org/10.1016/j.apmr.2011.07.196 (2012).
43. Min, B. H. et al. Effects of low-intensity ultrasound (LIUS) stimulation on human cartilage explants. *Scand. J. Rheumatol.* **35**, https://doi.org/10.1080/03009740600588418 (2006).
44. Uddin, S. M. et al. Chondro-protective effects of low intensity pulsed ultrasound. *Osteoarthr. Cartil.* **24**, 1989–1998 (2016).
45. Yamaguchi, S. et al. Effect of low-intensity pulsed ultrasound after mesenchymal stromal cell injection to treat osteochondral defects: an in vivo study. *Ultrasound Med Biol.* **42**, 2903–2913 (2016).
46. Chung, C. & Burdick, J. A. Influence of three-dimensional hyaluronic acid microenvironments on mesenchymal stem cell chondrogenesis. *Tissue Eng. Part A* **15**, https://doi.org/10.1089/ten.tea.2008.0067 (2009).
47. Lee, Y. et al. Three-dimensional microenvironmental priming of human mesenchymal stem cells in hydrogels facilitates efficient and rapid retroviral gene transduction via accelerated cell cycle synchronization. *NPG Asia Mater.* **11**, https://doi.org/10.1038/s41427-019-0127-9 (2019).
48. Anderson-Baron, M. et al. Suppression of hypertrophy during in vitro chondrogenesis of cocultures of human mesenchymal stem cells and nasal chondrocytes correlates with lack of in vivo calcification and vascular invasion. *Front. Bioeng. Biotechnol.* **8**, 572356 (2020).
49. Macias, M. J., Martin-Malpartida, P. & Massague, J. Structural determinants of Smad function in TGF-beta signaling. *Trends Biochem. Sci.* **40**, 296–308 (2015).
50. Rothweiler, R. et al. Predicting and promoting human bone marrow MSC chondrogenesis by way of TGFbeta receptor profiles: toward personalized medicine. *Front. Bioeng. Biotechnol.* **8**, 618 (2020).
51. Park, J. S. et al. The effect of matrix stiffness on the differentiation of mesenchymal stem cells in response to TGF-beta. *Biomaterials* **32**, 3921–3930 (2011).
52. Ren, K. et al. Injectable polypeptide hydrogels with tunable microenvironment for 3D spreading and chondrogenic differentiation of bone-marrow-derived mesenchymal stem cells. *Biomacromolecules* **17**, 3862–3871 (2016).
53. Choi, B. et al. Covalently conjugated transforming growth factor-beta1 in modular chitosan hydrogels for the effective treatment of articular cartilage defects. *Biomater. Sci.* **3**, 742–752 (2015).
54. Jeong, C. G., Zhang, H. & Hollister, S. J. Three-dimensional polycaprolactone scaffold-conjugated bone morphogenetic protein-2 promotes cartilage regeneration from primary chondrocytes in vitro and in vivo without accelerated endochondral ossification. *J. Biomed. Mater. Res. A* **100**, 2088–2096 (2012).
55. Longo, U. G. et al. Osteoarthritis: new insights in animal models. *Open Orthop. J.* **6**, 558–563 (2012).
56. Teeple, E., Jay, G. D., Elsaid, K. A. & Fleming, B. C. Animal models of osteoarthritis: challenges of model selection and analysis. *AAPS J.* **15**, 438–446 (2013).
57. Cook, J. L. et al. Animal models of cartilage repair. *Bone Jt. Res.* **3**, 89–94 (2014).
58. Park, D. Y., Min, B.-H., Lee, H. J., Kim, Y. J. & Choi, B. H. Repair of partial thickness cartilage defects using cartilage extracellular matrix membrane-based chondrocyte delivery system in human ex vivo model. *Tissue Eng. Regenerative Med.* **13**, 182–190 (2016).
59. Zhang, W. et al. The use of type 1 collagen scaffold containing stromal cell-derived factor-1 to create a matrix environment conducive to partial-thickness cartilage defects repair. *Biomaterials* **34**, 713–723 (2013).
60. Nam, J., Perera, P., Rath, B. & Agarwal, S. Dynamic regulation of bone morphogenetic proteins in engineered osteochondral constructs by biomechanical stimulation. *Tissue Eng. Part A* **19**, 783–792 (2013).
61. Ozeki, N. et al. Not single but periodic injections of synovial mesenchymal stem cells maintain viable cells in knees and inhibit osteoarthritis progression in rats. *Osteoarthr. Cartil.* **24**, 1061–1070 (2016).
62. Solak, K. et al. Histological comparison of nanocomposite multilayer biomimetic scaffold, a chondral scaffold, and microfracture technique to repair experimental osteochondral defects in rats. *Eurasia. J. Med.* **52**, 145–152 (2020).
63. Kondo, M. et al. Safety and efficacy of human juvenile chondrocyte-derived cell sheets for osteochondral defect treatment. *NPJ Regen. Med.* **6**, 65 (2021).
64. Zhang, W. et al. Tannic acid-mediated dual peptide-functionalized scaffolds to direct stem cell behavior and osteochondral regeneration. *Chem. Eng. J.* **396**, https://doi.org/10.1016/j.cej.2020.125232 (2020).
65. McCall, J. D., Luoma, J. E. & Anseth, K. S. Covalently tethered transforming growth factor beta in PEG hydrogels promotes chondrogenic differentiation of encapsulated human mesenchymal stem cells. *Drug Deliv. Transl. Res.* **2**, 305–312 (2012).
66. Bourguignon, L. Y., Singleton, P. A., Zhu, H. & Zhou, B. Hyaluronan promotes signaling interaction between CD44 and the transforming growth factor beta receptor I in metastatic breast tumor cells. *J. Biol. Chem.* **277**, 39703–39712 (2002).
67. Bandow, K. et al. Low-intensity pulsed ultrasound (LIPUS) induces RANKL, MCP-1, and MIP-1beta expression in osteoblasts through the angiotensin II type 1 receptor. *J. Cell Physiol.* **211**, 392–398 (2007).
68. Wang, X. et al. Low-intensity pulsed ultrasound promotes chondrogenesis of mesenchymal stem cells via regulation of autophagy. *Stem Cell Res. Therapy* **10**, https://doi.org/10.1186/s13287-019-1142-z (2019).
69. Hiyama, A. et al. Synergistic effect of low-intensity pulsed ultrasound on growth factor stimulation of nucleus pulposus cells. *J. Orthop. Res.* **25**, 1574–1581 (2007).
70. Smeds, K. A. et al. Photocrosslinkable polysaccharides for in situ hydrogel formation. *J. Biomed. Mater. Res.* **54**, 115–121 (2001).